Electron Transfer on Insulator Surfaces: Exciplex Emission and the Role of Electron Diffusion in Determining Radical Deactivation Rates

David R. Worrall, Siân L. Williams, and Francis Wilkinson*

Department of Chemistry, Loughborough University, Loughborough, Leicestershire LE11 3TU, U.K.

Received: October 31, 1997; In Final Form: January 5, 1998

The kinetics of electron transfer on silica gel between the anthracene radical cation and the electron donors triphenylamine (TPA) and *N*,*N*,*N*′,*N*′-tetramethyl-1,4-phenylenediamine (TMPD) have been investigated using the technique of diffuse reflectance laser flash photolysis. The mean rate of decay of the anthracene radical cation, determined as the maximum of the rate constant distribution, correlates with the surface concentration of the electron donor in both cases up to a loading of 2 μmol g^{-1}. In the case of triphenylamine as donor, using 355 nm excitation, plots of mean electron-transfer rate constant versus electron-donor concentration deviate positively from linearity at higher donor concentrations. In the case of TMPD, linearity is preserved at higher loadings with 355 nm excitation, where TMPD does not absorb appreciably and is not therefore directly photoionized, but again a positive deviation ensues with 266 nm excitation that causes direct photoionization of TMPD. In both cases the increased rate of decay of the anthracene radical cation correlates with appreciable direct photoionization of the electron donor. The enhanced rate of decay is explained as being due to donor photoionization increasing the local concentration of electrons on the surface and electron diffusion competing efficiently with donor diffusion leading to increased anthracene radical cation decay. In addition, we have demonstrated the formation between anthracene and TPA coadsorbed on silica gel of an emissive exciplex and have found no evidence that relaxation of this exciplex results in radical ion pair formation.

Introduction

Electronically excited states of polynuclear aromatic hydrocarbons have been the subject of much study in solution[1−5] and, more recently, adsorbed on insulator surfaces.[6−16] Photochemical and photophysical studies of molecules adsorbed onto insulator surfaces can provide information concerning the strength of interactions between the surface and the probe, including the nature of adsorption sites and the mobility of the probe. Studies of molecules adsorbed on solid substrates have revealed that many molecules diffuse rapidly across the surface of silica gel and γ-alumina. Thus triplet−triplet annihilation,[6,17,18] dynamic excimer formation,[11] and energy[21,25] and electron transfer[7,25] have all been used to study the diffusion of adsorbates on surfaces.

The fate and residence time of polycyclic aromatic hydrocarbons in the environment are of great concern, and hence their heterogeneous reaction pathways are of more than academic interest. In addition, electron-transfer reactions in general are of great importance in both chemistry and biology, although there have been few direct studies of heterogeneous electron-transfer dynamics. Photoinduced electron transfer on surfaces is of particular importance in the area of heterogeneous catalysis and in particular the use of metal oxides including active supports such as TiO_2 in applications such as wastewater treatment.[26] As has been shown in previous publications,[6−25,27−38] insulator supports such as silica gel provide an environment that can stabilize reaction intermediates that are very short-lived in solution and as such render them amenable to convenient study. As a consequence, a detailed study of the kinetics of the electron-transfer reactions of photoproduced radical cations on silica gel provides a unique insight into the controlling factors in these reactions.

The formation of arene radical cations on insulator supports following laser excitation has been reported by several authors including ourselves.[6−25,27−38] The mechanism of their production is dependent upon both the nature of the interactions between the surface onto which the molecule of interest is adsorbed and on the molecule concerned. Using laser dose studies, the formation of arene radical cations, including distyrylbenzene[19] adsorbed onto both silica gel and γ-alumina and pyrene[8,25] on γ-alumina, have been shown to be via bi- or multiphoton processes. The production of arene radical cations within zeolites is more complicated due to the varied nature of the adsorption sites and the presence of alkali-metals cations, such as sodium and copper. Pyrene,[33,35] anthracene,[33,37] naphthalene,[37] and *trans*-stilbene[37] radical cations are produced by both mono- and biphotonic mechanisms when included within zeolites. We have shown previously that excitation of anthracene adsorbed on silica gel at 355 nm readily forms, by a multiphotonic process,[6] the radical cation, which has been identified as such by its characteristic absorption spectrum.[39,40] In a previous publication[7] we reported electron transfer to the anthracene radical cation from a range of electron donors, *N*,*N*,*N*′,*N*′-tetramethyl-1,4-phenylenediamine (TMPD), azulene, triphenylamine (TPA), and *N*,*N*-dimethylaniline (DMA) when coadsorbed with anthracene on silica gel. For all of the above compounds a linear correlation between the observed electron-transfer rates and electron-donor concentration was seen up to a loading of 2 μmol g^{-1}. In this paper we present data showing that at higher concentrations of triphenylamine and TMPD, under appropriate conditions of photoexcitation, a positive

S1089-5639(98)00044-9 CCC: $15.00

deviation from linearity is seen and the rate of electron transfer increases disproportionately with increasing electron-donor concentration.

Previously[6] we reported the formation of an emissive anthracene excimer on the surface of silica gel. Three peaks were observed in the emission spectrum of anthracene adsorbed on silica gel at 400, 450, and 530 nm, which were assigned as due to delayed fluorescence, excimer emission, and emission from protonated anthracene, respectively. Exciplex emission on silica gel has been observed with anthracene coadsorbed with aromatic amines such as *N*,*N*-diethylaniline and *N*,*N*-dimethylaniline by Eremenko and co-workers.[41−44] Such exciplexes formed between anthracene and *N*,*N*-dimethylaniline can also be formed in cyclohexane solution.[45] Transient absorption studies in solution have provided evidence for the formation of triphenylamine exciplexes with various quinones.[46−51] In this publication we present results obtained from laser-induced transient emission studies of TPA coadsorbed with anthracene on silica gel and report the first observation of emission from an anthracene/TPA exciplex.

Experimental Section

Samples of anthracene on silica gel were prepared according to the method described previously in detail in ref 6. Briefly, silica gel (Davisil grade 635, Aldrich Chemical Co.) was dried at 125 °C under vacuum to 5×10^{-5} mbar, and the vessel repressurized with dry nitrogen. Anthracene (scintillation grade, Sigma) was dissolved in *n*-hexane or acetonitrile (spectrophotometric grade, Aldrich Chemical Co.) previously dried by reflux over calcium hydride (reagent grade, Fisons), and the resulting solution added to the dried silica gel. After equilibration for 3 h, the excess solution was decanted off and the sample dried under vacuum to 5×10^{-5} mbar. The sample was then sealed into a cylindrical glass or quartz cuvette (22 mm diameter × 10 mm path length). Sample loadings were determined from the reduction in absorption of the UV−vis spectrum of the decanted solution compared to the spectrum of the solution prior to exposure to the silica gel. The incorporation of electron donors in the anthracene/silica system was achieved by the addition of the donor to the anthracene solution prior to addition to the dried silica gel. Sample loadings of the electron donors were in the range 0.1−10 μmol g^{-1}, corresponding to a homogeneous 2D surface concentration range of 0.005−0.5% of a monolayer, while the anthracene concentration was kept constant at 0.5 μmol g^{-1}, corresponding to a homogeneous 2D surface concentration of 0.025%.

The nanosecond diffuse reflectance laser flash photolysis apparatus has been described previously in detail in ref 52. Excitation of the samples was either with the third (355 nm, 11 mJ/pulse) or the fourth harmonic (266 nm, 27 mJ/pulse) of a Lumonics HY200 HyperYAG Nd:YAG laser. Diffusely reflected analyzing light from a 275 W xenon arc lamp (Oriel) was collected and focused onto the slit of an *f*/3.4 grating monochromator (Applied Photophysics) and detected with a side-on photomultiplier tube (Hamamatsu R928). Signal capture was either by a 2432A digital oscilloscope (Tektronix) or Model 9845 transient digitizing card (EG&G), both interfaced to an IBM-compatible PC.

Time-resolved emission measurements were carried out following laser excitation using the third harmonic of a Lumonics HyperYAG Nd:YAG laser (355 nm, 11 mJ/pulse). Collection of the emitted light was via a fused-silica fiber bundle in contact with the entrance slit of a gated photodiode array system (EG&G Princeton Applied Research, Model 1235 digital grating spectrograph, gratings blazed for 300 and 500 nm, with a Model 1455 peltier cooled linear photodiode array detector and a Model 1461 detector controller) interfaced to an IBM-compatible PC.

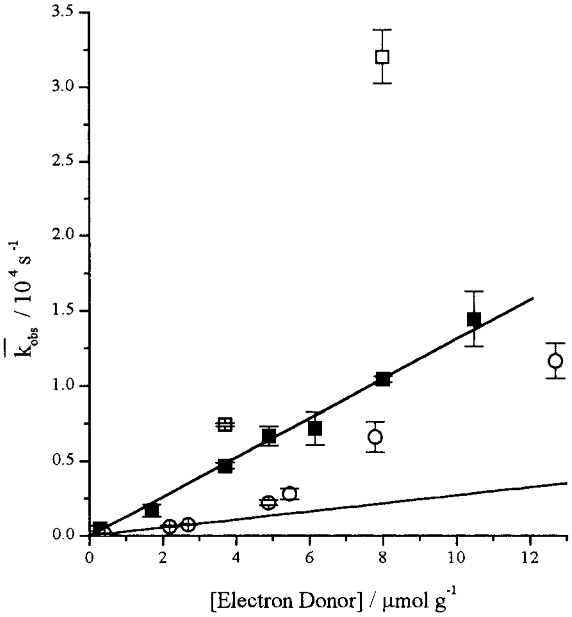

Figure 1. Variation in the mean rate constant (k_{obs}) for electron transfer from electron donors, TMPD (■) and TPA (○) following excitation at 355 nm and TMPD (□) following excitation at 266 nm, to the anthracene radical cation as a function of electron donor concentration.

Results and Discussion

(i) Kinetics of Electron Transfer. The anthracene radical cation is formed following laser excitation, at 355 nm, of anthracene adsorbed on silica gel[6,7] through multiphoton absorption. The decay kinetics of the anthracene radical cation adsorbed alone on silica gel do not conform to a single exponential; the decay is complex, with components on time scales ranging from microseconds to hours. At early times and low loadings the decay can be fitted successfully with a model that assumes geminate recombination to be the primary deactivation pathway.[7] The coadsorption of an electron donor with anthracene on silica gel causes an increase in the rate of decay of the anthracene radical cation, provided that the oxidation potential of the electron donor is less than 1.09 V (vs SCE), which is the reduction potential of the anthracene radical cation.[53]

In the presence of coadsorbed electron donors the decay kinetics of the anthracene radical cation are again complex and do not conform to a single-exponential decay. A model that has been used by us[7] and others[22,25,54−62] to describe the kinetics of reactions on surfaces, including electron transfer on silica gel, is a dispersive kinetic model that assumes a distribution of rate constants for the observed reaction.[63] We have applied this model to kinetic data obtained for electron transfer on silica gel from an electron donor to the anthracene radical cation[7] and have shown that plots of observed mean electron-transfer rate versus coadsorbed donor concentration are linear for each of the electron donors studied up to a loading of 2 μmol g^{-1}. The intercepts of such plots are zero (within experimental error), demonstrating that electron transfer is the dominant decay pathway. Beyond a loading of 2 μmol g^{-1} for TMPD with 355 nm excitation, these plots remain linear. However, in the case of TPA a positive deviation from linearity is observed (Figure 1).

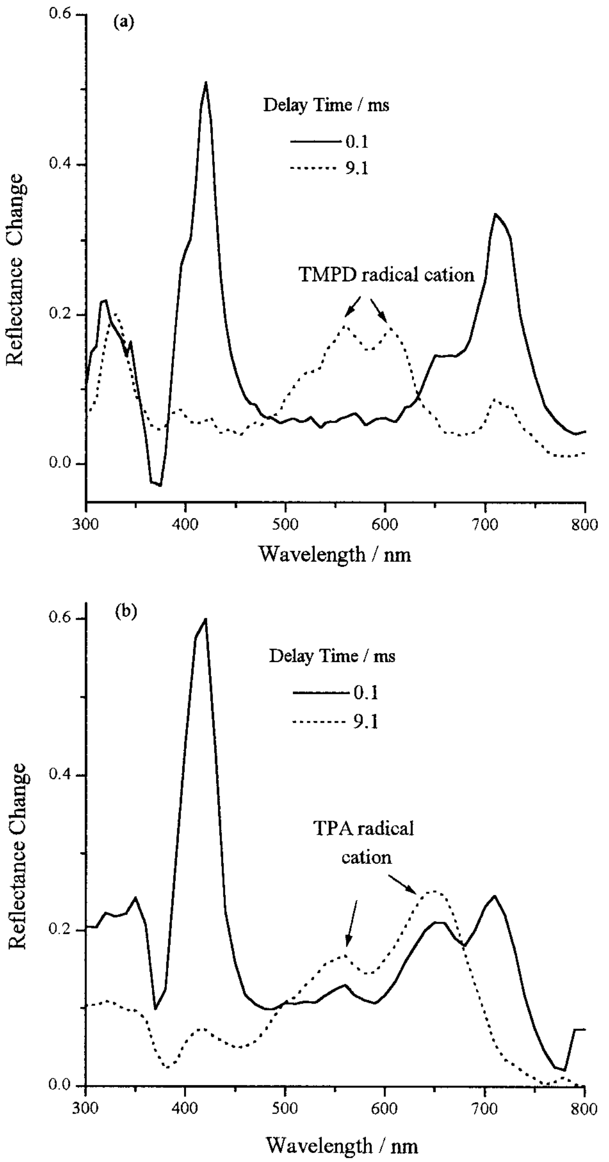

Figure 2. Transient absorption spectra of (a) anthracene coadsorbed with TMPD and (b) anthracene coadsorbed with TPA at delays of 0.1 and 9.1 ms following laser excitation at 355 nm. Laser pulse energy 11 mJ cm^{-2}.

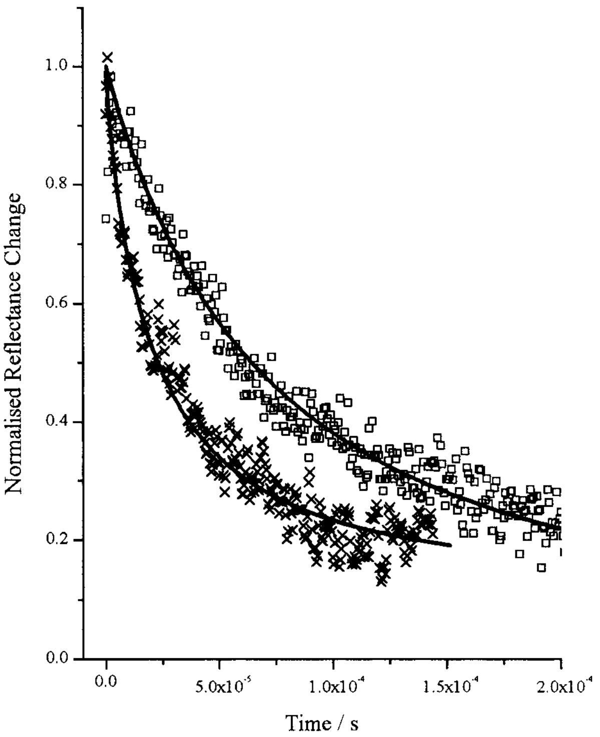

Figure 3. Time-resolved transient absorption at 715 nm of anthracene coadsorbed with TMPD on silica gel exciting at (□) 355 nm and (×) 266 nm.

Inspection of the transient difference spectra of anthracene coadsorbed with TMPD and TPA immediately following excitation at 355 nm reveals an interesting difference. In the case of anthracene with TMPD, immediately following excitation there is no absorption attributable to the TMPD radical cation (Figure 2a). However, in the case of anthracene with TPA the earliest transient spectra, i.e., within 50 ns of the laser pulse show appreciable absorption due to the radical cation of TPA. It should be noted that kinetic data were gathered at a sampling rate of up to and including 200 MHz with a record length in excess of 16 000 points in order to sample both fast and slow transient features. Figure 2 shows a comparison of the transient absorption spectra of TPA and TMPD coadsorbed with anthracene, demonstrating that while the TMPD radical cation is essentially absent 0.1 ms following laser excitation, the TPA radical cation has appreciable population after this time. This rapidly formed TPA radical cation signal shows no rise kinetics on a time scale of less than 100 ns and hence cannot arise from diffusional electron transfer to the anthracene radical cation. Indeed as shown in a previous publication[7] the relative rates of electron transfer of TPA and TMPD to the anthracene radical cation are different by only a factor of 3, with TPA giving the slower electron-transfer rate; this again indicates that the rapidly formed TPA radical cation is not formed as a result of diffusional electron transfer. Flash photolysis of a sample of TPA adsorbed alone on silica gel shows that the promptly formed radical cation absorption is the result of ionization following the absorption of 355 nm radiation. It should be noted that it is not possible to comment on the relative yields of promptly formed donor and acceptor radical cations in these experiments, since competitive ground-state absorption is not the only factor involved in determining the observed yield. Also involved are the excited-state absorptions involved in the consecutive two-photon ionization process, absorption of the excitation wavelength by the triplet state of anthracene, and aggregation effects at higher loadings which make accurate interpretation of the ground-state absorption profiles difficult. In addition, there is a strong overlap of the radical cation absorption spectra of anthracene and TPA, which further complicates analysis.

In the case of TMPD adsorbed alone on silica gel, excitation at 355 nm results in negligible TMPD radical cation formation. However, excitation at 266 nm results in the formation of the TMPD radical cation in amounts comparable to 355 nm photolysis of TPA. Prompt formation of the TMPD radical cation is observed in the transient absorption spectra of TMPD coadsorbed with anthracene when 266 nm is used as the excitation wavelength. Excitation of anthracene coadsorbed with TMPD at 266 nm yields a decay of the anthracene radical cation faster than that observed for the same samples following excitation at 355 nm (Figure 3). This difference in rates is illustrated as a function of TMPD concentration in Figure 1, where the kinetics of decay following 266 nm excitation are shown as hollow squares. Clearly there is a strong positive deviation from linearity with increasing TMPD loading with the rate of anthracene radical cation deactivation increasing

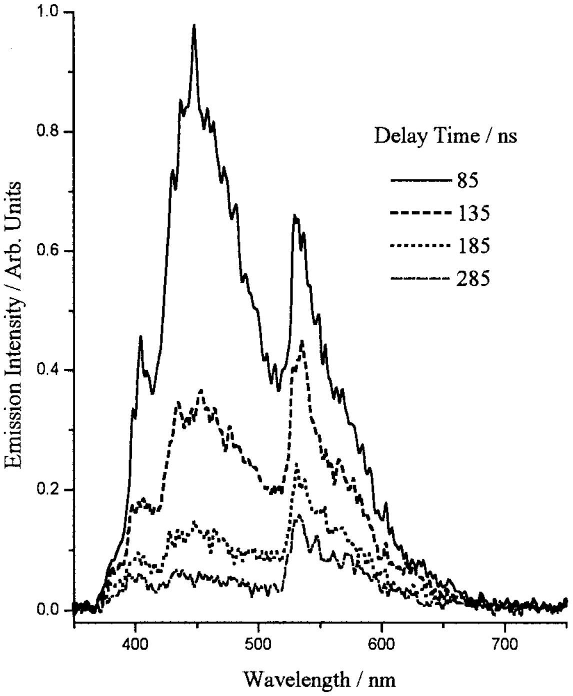

Figure 4. Time-resolved transient emission spectra of anthracene adsorbed on silica gel following laser excitation at 355 nm. Sample loading 1.7 μmol g^{-1}. Integration time 100 ns. Laser pulse energy 11 mJ cm^{-2}.

disproportionately as TMPD concentration increases when excitation is at 266 nm. This behavior is similar to that seen for the anthracene/TPA system when exciting at 355 nm, the behavior of which with TPA loading is also shown in Figure 1. Experiments with anthracene adsorbed alone on silica gel have shown that the kinetics of decay of the anthracene radical cation are independent of the excitation wavelength. Silica gel itself shows no transient absorption when excited at 266 nm. Both of these observations clearly indicate that it is the direct photoionization of the TMPD which is responsible for the acceleration in the decay rate of the anthracene radical cation.

(ii) Time-Resolved Emission Measurements. Time-resolved emission measurements have been carried out with anthracene coadsorbed with the electron donors on silica gel. Detection was with a gated photodiode array spectrometer with a 100 ns gate width, the gate being triggered after the 355 nm exciting laser pulse in order to exclude prompt anthracene fluorescence. Previous time-resolved emission studies of anthracene adsorbed alone on silica gel have revealed the presence of three emission peaks.[6] Figure 4 shows a typical spectrum, the three peaks being assigned as delayed fluorescence peaking at 400 nm, excimer emission (450 nm), and emission from protonated anthracene (530 nm). Coadsorption of TMPD has no effect on the observed transient emission spectrum over the range of TMPD loadings employed. Coadsorption of TPA, on the other hand, produces a profound change in the observed transient emission spectra. The wavelengths of the peaks corresponding to delayed fluorescence and protonated anthracene emission remain unchanged; however, the peak at 450 nm assigned previously as excimer emission disappears and is replaced by a peak at 500 nm (Figure 5). This decrease in excimer emission intensity with increasing TPA loading implies either dynamic competition with excimer formation or preferential TPA adsorption in a region near where the anthracene is adsorbed. In the former case, TPA diffusion could compete efficiently with anthracene diffusion for interception of excited singlet-state anthracene molecules. Inspection of the emission spectra as a function of TPA loading shows that appreciable exciplex formation occurs when the TPA concentration is comparable with that of the anthracene, implying similar rate constants for the formation of both excimer and exciplex. If a static mechanism is responsible, then due to the low average surface coverages (less than 3% of a monolayer), adsorption of TPA and anthracene in close proximity is required. Experiments are currently underway to attempt to distinguish between these two possibilities. The intensity of the 500 nm peak increases with increasing TPA loading (Figure 6). The decay of the emission at 500 nm seen with anthracene coadsorbed with TPA decays with a first half-life of 33 ± 10 ns and shows an approximately single-exponential decay, which is the same within experimental error as the 30 ± 10 ns lifetime found for the anthracene excimer emission determined with anthracene adsorbed alone on silica gel. This emission at 500 nm is assigned, on the basis of its intensity behavior as a function of TPA loading, as due to an exciplex formed between anthracene and TPA. Such exciplex emission at similar wavelengths has been observed previously for anthracene and other tertiary amines by Eremenko et al.[41] In the case of TPA, exciplex formation is accompanied by a decrease in prompt anthracene fluorescence intensity with increasing TPA loading (Figure 7), which is as expected since exciplex formation necessarily decreases the surface population of free excited singlet-state anthracene. Inspection of the transient absorption immediately following the laser pulse reveals no increase in TPA radical absorption on the time scale of the relaxation of the exciplex, clearly demonstrating that the exciplex dissociates to give the neutral ground states of anthracene and TPA rather than to a radical ion pair.

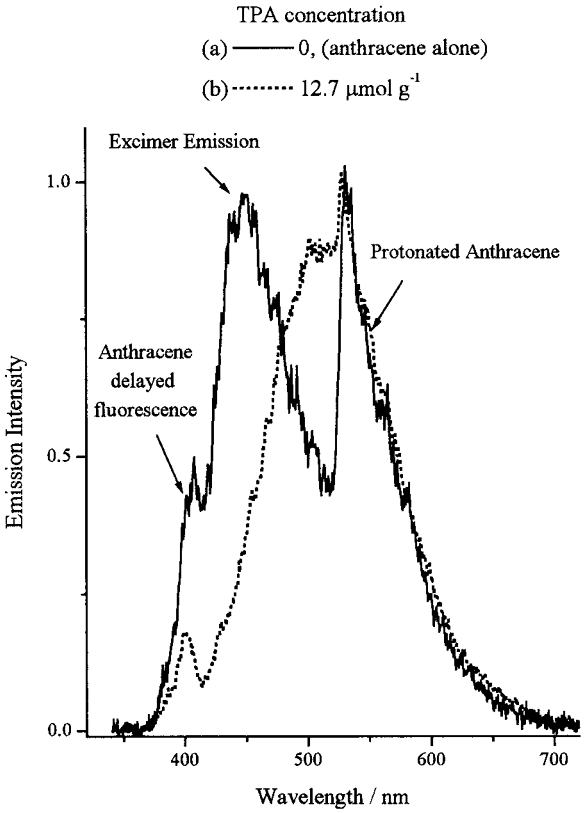

Figure 5. Normalized transient emission spectra of (a) anthracene alone and (b) anthracene coadsorbed with TPA on silica gel following laser excitation at 355 nm. Integration time 100 ns. Laser pulse energy 11 mJ cm^{-2}.

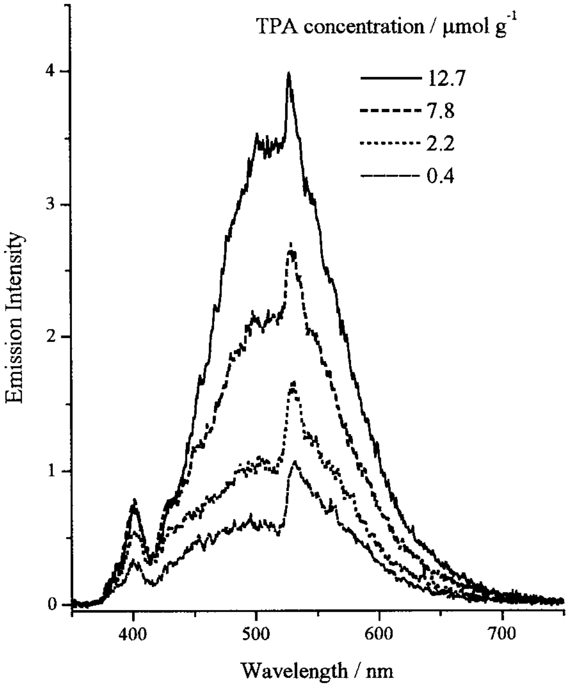

Figure 6. Transient emission spectra of anthracene coadsorbed with TPA on silica gel following laser excitation at 355 nm as a function of TPA concentration. Integration time 100 ns. Laser pulse energy 11 mJ cm^{-2}.

A Proposed Mechanism

The proposed mechanism for the enhancement in electron-transfer rate at high surface concentrations of TPA when excited at 355 nm and of TMPD when excited at 266 nm is shown schematically below (here D denotes electron donor, either TPA or TMPD):

$$\mathrm{An} + h\nu \rightarrow \mathrm{An}^*(\mathrm{S}_1) \qquad \text{excitation} \qquad \text{(i)}$$

$$\mathrm{An}^*(\mathrm{S}_1) + h\nu \rightarrow \mathrm{An}^{\bullet+} + \mathrm{e}^- \qquad \text{ionization (due to absorption of second photon)} \qquad \text{(ii)}$$

$$\mathrm{D} + nh\nu \rightarrow \mathrm{D}^{\bullet+} + \mathrm{e}^- \qquad \text{photoionization of electron donor} \qquad \text{(iii)}$$

$$\mathrm{An}^{\bullet+} + \mathrm{D} \rightarrow \mathrm{An} + \mathrm{D}^{\bullet+} \qquad \text{electron transfer} \qquad \text{(iv)}$$

$$\mathrm{An}^{\bullet+} + \mathrm{e}^- \rightarrow \mathrm{An} \qquad \text{ion–electron combination} \qquad \text{(v)}$$

$$\mathrm{An}^*(\mathrm{S}_1) + \mathrm{An} \rightarrow [\mathrm{An...An}]^* \qquad \text{excimer formation} \qquad \text{(vi)}$$

$$[\mathrm{An...An}]^* \rightarrow \mathrm{An} + \mathrm{An} + h\nu \qquad \text{excimer emission} \qquad \text{(vii)}$$

The following steps are only observed for TPA:

$$\mathrm{An}^*(\mathrm{S}_1) + \mathrm{TPA} \rightarrow [\mathrm{An}\cdots\mathrm{TPA}]^* \qquad \text{exciplex formation} \qquad \text{(viii)}$$

$$[\mathrm{An}\cdots\mathrm{TPA}]^* \rightarrow \mathrm{An} + \mathrm{TPA} + h\nu \qquad \text{exciplex emission} \qquad \text{(ix)}$$

$$[\mathrm{An}\cdots\mathrm{TPA}]^* \rightarrow \mathrm{An} + \mathrm{TPA} \qquad \text{exciplex dissociation} \qquad \text{(x)}$$

For simplicity, triplet-state reactions are not included in the above scheme. Under circumstances where direct ionization of the electron donor is small, such as with TMPD (with 355 nm excitation), step iv is very much faster than step v, and consequently a linear correlation between radical cation deactivation rate and donor concentration is observed. Where formation of the electron-donor cation through direct laser excitation is appreciable, step iii acts to increase the free electron concentration at or near the silica surface. This high local concentration allows ion–electron recombination (step v) to proceed at a faster rate than electron transfer (step iv) as an anthracene radical cation deactivation mechanism. In addition, the reduction potentials of the anthracene and TPA radical cations are such that ion–electron recombination between the anthracene radical cation and the surface electron is energetically favored over that between the TPA radical cation and the surface electron. An additional consideration is the depth of the surface trap in which the electron produced in step iii finds itself. In the photoionization scheme without direct photoionization of the donor, only those radicals whose ejected electrons that find relatively high energy traps are long-lived; those whose electrons are weakly bound to the surface will rapidly undergo back-electron transfer. In the case of appreciable donor photoionization, step iii produces electrons on the surface that may be stable even though relatively weakly bound, as a result of the lower reduction potential of the TPA radical cation. Such electrons in "shallow" surface traps may be expected to recombine more readily with any locally produced anthracene radical cations rather than with TPA radical cations due to the free energy (ΔG) for combination of these electrons with the anthracene radical cation being more negative than that for TPA, assuming that the rate of ion–electron combination correlates with the magnitude of the free energy for the electron-transfer process. Step iii, photoionization of the electron donor, explains the observed formation of the TPA radical cation before diffusion of TPA to photoionized anthracene molecules has made a significant contribution and also the prompt formation of the TMPD radical cation with 266 nm excitation.

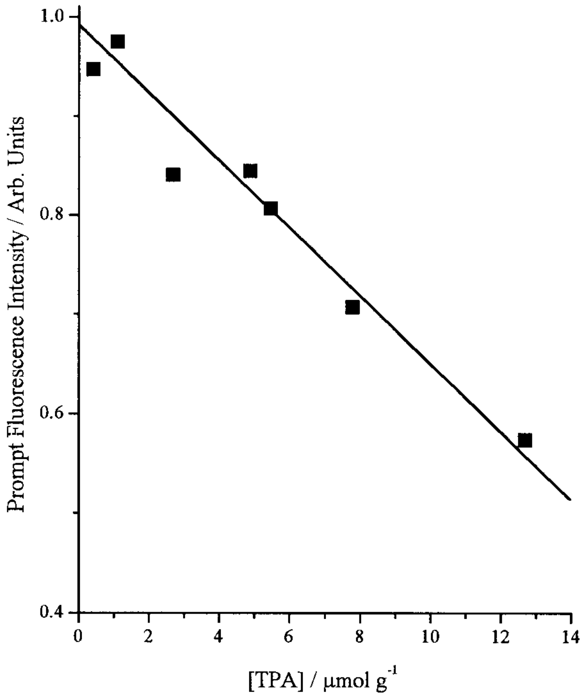

Figure 7. Prompt fluorescence intensity monitored at 400 nm of anthracene coadsorbed with TPA on silica gel versus TPA concentration.

This mechanism is supported by the data obtained with the same samples containing anthracene and TMPD comparing the decay kinetics of the anthracene radical cation excited at 355 nm where direct photoionization of TMPD does not occur and excited at 266 nm where direct photoionization is appreciable. The marked increase in the rate of decay of the anthracene radical cation following excitation at 266 nm is explained by the presence of free electrons on the surface produced by direct photoionization of TMPD, leading to electron−anthracene radical cation combination. We have demonstrated that the kinetics of ion−electron recombination for anthracene adsorbed alone on silica gel are insensitive to excitation wavelength. Clearly if this mechanism is operative, there should be a laser energy dependence of the free-electron concentration on the surface and hence on the anthracene radical decay kinetics. However, attempts at laser dose studies have proved unsuccessful since reduction in laser energy results in a marked decrease in reflectance change due to the multiphotonic nature of the transient production, and consequently there is a marked increase in the error associated with the fitted parameters, and systematic changes in the mean rate constant are impossible to discern. Increasing laser energy results in reflectance changes of greater than 10−15%, which results in nonlinearities of reflectance change versus concentration.[64,65] We are currently investigating other electron donor−acceptor systems in order to clarify this proposed mechanism.

Conclusions

For anthracene with TPA coadsorbed on silica gel, the observed rate of electron transfer to the anthracene radical cation does not show a simple linear relationship with increasing electron donor concentration at higher loadings. It is suggested that since direct photoionization of TPA occurs at higher concentration, this creates a high local concentration of electrons on the surface and consequently back-electron-transfer becomes faster than surface diffusion under these conditions. In addition, the first exciplex emission from an anthracene/TPA exciplex has been reported, with a lifetime of 33 ± 10 ns on the surface of silica gel. Relaxation of the exciplex does not contribute to the overall radical kinetics. The observation of the wavelength dependence on the anthracene radical cation decay kinetics in the presence of TMPD and the onset of nonlinearities in the anthracene radical cation decay in the presence of higher loadings of TPA when excited at 355 nm demonstrates that where direct photoionization on the surface is appreciable electron diffusion can dominate over molecular diffusion. The possibility that this mechanism may operate must be borne in mind when interpreting data from other donor-acceptor systems.

Acknowledgment. The authors wish to thank EPSRC for financial support and Mr. A. Tredgett, Mrs. S. Wilson, and Miss F. Delepine for their help in the preparation of some samples.

References and Notes

(1) Wilkinson, F.; McGarvey, D. J.; OLea, A. F. *J. Am. Chem. Soc.* **1993**, *115*, 12144.

(2) Wang, Z.; Weininger, S. J.; McGimpsey, W. G. *J. Phys. Chem.* **1993**, *97*, 374.

(3) Chakraborty, T.; Lim, E. C. *J. Phys. Chem.* **1993**, *97*, 11151.

(4) McVey, J. K.; Should, D. M.; Yang, N. C. *J. Phys. Chem.* **1976**, *65*, 3375.

(5) Mataga, N.; Torihashi, Y.; Ota, Y. *Chem. Phys. Lett.* **1967**, *1*, 385.

(6) Wilkinson, F.; Worrall, D. R.; Williams, S. L. *J. Phys. Chem.* **1995**, *99*, 6689.

(7) Worrall, D. R.; Williams, S. L.; Wilkinson, F. *J. Phys. Chem. B.* **1997**, *101*, 4709.

(8) Beck, G.; Thomas, J. K. *Chem. Phys. Lett.* **1983**, *94*, 553.

(9) Dabestani, R.; Ellis, K. J.; Sigman, M. E. *J. Photochem. Photobiol. A Chem.* **1995**, *86*, 231.

(10) Bjarneson, D. W.; Peterson, N. O. *J. Am. Chem. Soc.* **1990**, *112*, 988.

(11) Bauer, R. K.; de Mayo, P.; Natarajan, L. V.; Ware, W. R. *Can. J. Chem.* **1984**, *62*, 1279.

(12) Bauer, R. K.; Borenstein, R.; deMayo, P.; Okada, K.; Rafalska, M.; Ware, W. R.; Wu, K. C. *J. Am. Chem. Soc.* **1982**, *104*, 4635.

(13) Fujii, T.; Ishii, A.; Satozono, H.; Suzuki, S.; Takusagawa, N.; Anpo, M. J. *Photochem. Photobiol. A: Chem.* **1994**, *84*, 283.

(14) Fujii, T.; Ishii, A.; Takusagawa, N.; Yamashita, H.; Anpo, M. J. *J. Photochem. Photobiol. A: Chem.* **1995**, *86*, 219.

(15) Hayashi, Y.; Kawada, Y.; Ichimura, K. *Langmuir* **1995**, *11*, 2077.

(16) Mao, Y.; Iu, K.-K.; Thomas, J. K. *Langmuir* **1994**, *10*, 709.

(17) Oelkrug, D.; Uhl, S.; Wilkinson, F.; Willsher, C. J. *J. Phys. Chem.* **1989**, *93*, 4551.

(18) Oelkrug, D.; Gregor, M.; Reich, S. J. *Photochem. Photobiol.* **1991**, *54*, 539.

(19) Oelkrug, D.; Reich, S.; Wilkinson, F.; Leicester, P. A. *J. Phys. Chem.* **1991**, *95*, 269.

(20) Frederick, B.; Johnston, L. J.; de Mayo, P.; Wong, S. K. *Can. J. Chem.* **1984**, *62*, 403.

(21) Lednev, I. K.; Mathivanan, N.; Johnston, L. J. *J. Phys. Chem.* **1994**, *98*, 11444.

(22) Pankasem, S.; Thomas, J. K. *J. Phys. Chem.* **1991**, *95*, 7385.

(23) Oelkrug, D.; Krabichler, G.; Honnen, W.; Wilkinson, F.; Willsher, C. J. *J. Phys. Chem.* **1988**, *92*, 3589.

(24) Mao, Y.; Thomas, J. K. *Langmuir* **1992**, *8*, 2501.

(25) Pankasem, S.; Thomas, J. K. *J. Phys. Chem.* **1991**, *95*, 6990.

(26) Legrini, O.; Oliveros, E.; Braun, A. M. *Chem. Rev.* **1993**, *93*, 671.

(27) Iu, K.-K.; Thomas, J. K. *Langmuir* **1990**, *6*, 471.

(28) Johnston, L. J.; Scaiano, J. C.; Shi, J.-L.; Siebrand, W.; Zerbetto, F. *J. Phys. Chem.* **1991**, *95*, 10018.

(29) Ramamurthy, V.; Sanderson, D. R.; Eaton, D. F. *J. Phys. Chem.* **1993**, *97*, 13380.

(30) Park, J.; Kang, W.-K.; Ryoo, R.; Jung, K.-H.; Jang, D.-J. *J. Photochem. Photobiol. A: Chem.* **1994**, *80*, 333.

(31) Hashimoto, S.; Fukazawa, N.; Fukumura, H.; Masuhara, H. *Chem. Phys. Lett.* **1994**, *219*, 445.

(32) Kelly, G.; Willsher, C. J.; Wilkinson, F.; Netto-Ferreira, J. C.; Olea, A.; Weir, D.; Johnston, L. J.; Scaiano, J. C. *Can. J. Chem.* **1990**, *68*, 812.

(33) Iu, K. K.; Thomas, J. K. *J. Phys. Chem.* **1991**, *95*, 506.

(34) Liu, X.; Thomas, J. K. *Langmuir* **1993**, *9*, 727.

(35) Liu, X.; Iu, K.-K.; Thomas, J. K. *Chem. Phys. Lett.* **1993**, *204*, 163.

(36) Iu, K.-K.; Liu, X.; Thomas, J. K. *J. Phys. Chem.* **1993**, *97*, 8165.

(37) Iu, K.-K.; Liu, X.; Thomas, J. K.*J. Photochem. Photobiol. A: Chem.* **1994**, *79*, 103.

(38) Liu, X.; Iu, K.-K.; Thomas, J. K.; He, H.; Klinowski, J. *J. Am. Chem. Soc.* **1994**, *116*, 11811.

(39) Shida, T.; Iwata, S. *J. Am. Chem. Soc.* **1973**, *95*, 3473.

(40) Shida, T. *Physical Sciences Data 34, Electronic Absorption Spectra of Radical Ions;* Elsevier Science: Amsterdam, 1988.

(41) Yakimova, O. I.; Eremenko, A. M.; Chuiko, A. A. *J. Mol. Struct.* **1990**, *218*, 447.

(42) Eremenko, A. M.; Smirnova, N. P.; Samchuk, S. A.; Chujko, A. A. *Colloids and Surf.* **1992**, *63*, 83.

(43) Eremenko, A. M.; Chujko, A. A. *Res. Chem. Intermediates* **1993**, *19*, 375.

(44) Eremenko, A. M.; Kondilenko, V. P.; Lyuksutova, O. I.; Smirnova, N. P.; Tarasov, I. G.; Kikteva, T. A.; Ogenko, V. M. *Proc. Indian Acad. Sci. (Chem. Sci.)* **1996**, *107*, 779.

(45) Bera, P. K.; Nath, D.; Misra, A. J.; Chowdhury, M. *J. Photochem. Photobiol. A: Chem.* **1996**, *95*, 127.

(46) Levin, P. P.; Pluzhnikov, P. F.; Kuzmin, V. A. *Chem. Phys. Lett.* **1988**, *152*, 409.

(47) Levin, P. P.; Raghavan, P. K. N.; Kuzmin, V. A. *Chem. Phys. Lett.* **1990**, *167*, 67.

(48) Levin, P. P.; Raghavan, P. K. N. *Chem. Phys. Lett.* **1991**, *182*, 663.

(49) Levin, P. P.; Pluzhnikov, P. F.; Kuzmin, V. A. *Chem. Phys. Lett.* **1988**, *147*, 283.

(50) Levin, P. P.; Pluzhnikov, P. F.; Kuzmin, V. A. *Chem. Phys. Lett.* **1988**, *152*, 409.

(51) Amouyal, E.; Bensasson, R. *J. Chem. Soc., Faraday Trans. 1* **1977**, *73*, 1561.

(52) Wilkinson, F.; Kelly, G. P.; In *Handbook of Organic Photochemistry*; Scaiano, J. C., Ed.; CRC Press: Boca Raton, FL, 1989; Vol. 1, pp 293−314.

(53) Murov, S. L.; Carmichael, I.; Hug, G. L. *Handbook of Photochemistry*, 2nd ed.; Marcel Dekker: New York, 1993; Table 10b-2. Data taken from: Pysh, E. S.; Yang, N. C. *J. Am. Chem. Soc.* **1963**, *85*, 2124.

(54) Levin, P. P.; Katalnikov, I. V.; Ferreira, L. F. V.; Costa, S. M. B. *Chem. Phys. Lett.* **1992**, *193*, 461.

(55) Levin, P. P.; Costa, S. M. B.; Ferreira, L. F. V. *J. Photochem. Photobiol. A: Chem.* **1994**, *82*, 137.

(56) Levin, P. P.; Costa, S. M. B.; Ferreira, L. F. V. *J. Phys. Chem.* **1995**, *99*, 1267.

(57) Hite, P.; Krasnansky, R.; Thomas, J. K. *J. Phys. Chem.* **1986**, *90*, 5795.

(58) Krasnansky, R.; Koike, K.; Thomas, J. K. *J. Phys. Chem.* **1990**, *94*, 4521.

(59) Liu, X.; Thomas, J. K. *Langmuir* **1993**, *9*, 727.

(60) Iu, K.-K.; Liu, X.; Thomas, J. K. *J. Phys. Chem.* **1993**, *97*, 8165.

(61) Liu, X.; Mao, Y.; Reutten, S. A.; Thomas, J. K. *Solar Energy Mat. Solar Cells* **1995**, *38*, 199.

(62) Mao, Y.; Breen, N. E.; Thomas, J. K. *J. Phys. Chem.* **1995**, *99*, 9909.

(63) Albery, W. J.; Bartlett, P. N.; Wilde, C. P.; Darwent, J. R. *J. Am. Chem. Soc.* **1985**, *107*, 1854.

(64) Lin, T.-P.; Kan, H. K. A. *J. Opt. Soc. Am.* **1970**, *60*, 1252.

(65) Kessler, R. W.; Krabichler, G.; Uhl, S.; Oelkrug, D.; Hagan, W. P.; Hyslop, J.; Wilkinson, F. *Opt. Acta* **1983**, *30*, 1099.